BIOCHEMISTRY
including biophysical chemistry & molecular biology
Article

Biochemistry **2009,** *48,* 10637–10643 10637
DOI: 10.1021/bi901334b

Requirement of a Unique Ca^{2+}-Binding Loop for Folding of Tk-Subtilisin from a Hyperthermophilic Archaeon[†,‡]

Yuki Takeuchi,[§] Shun-ichi Tanaka,[§] Hiroyoshi Matsumura,[∥,⊥] Yuichi Koga,[§] Kazufumi Takano,[§,⊥] and Shigenori Kanaya*[,§]

[§]*Department of Material and Life Science and* [∥]*Department of Applied Chemistry, Graduate School of Engineering, Osaka University, 2-1 Yamadaoka, Suita, Osaka 565-0871, Japan, and* [⊥]*CREST, JST, 2-1 Yamadaoka, Suita, Osaka 565-0871, Japan*

Received August 1, 2009; Revised Manuscript Received October 8, 2009

ABSTRACT: Tk-subtilisin from the hyperthermophiolic archaeon *Thermococcus kodakaraensis* matures from Pro-Tk-subtilisin upon autoprocessing and degradation of Tk-propeptide [Tanaka, S., Saito, K., Chon, H., Matsumura, H., Koga, Y., Takano, K., and Kanaya, S. (2007) *J. Biol. Chem. 282*, 8246−8255]. It requires Ca^{2+} for folding and assumes a molten globule-like structure in the absence of Ca^{2+} even in the presence of Tk-propeptide. Tk-subtilisin contains seven Ca^{2+}-binding sites. Four of them (Ca2−Ca5) are located within a long loop, which mostly consists of a unique insertion sequence of this protein. To analyze the role of this Ca^{2+}-binding loop, three mutant proteins, Δloop-Tk-subtilisin, ΔCa2-Pro-S324A, and ΔCa3-Pro-S324A, were constructed. These proteins were designed to remove the Ca^{2+}-binding loop, Ca2 site, or Ca3 site of Pro-Tk-subtilisin or its active site mutant Pro-S324A. Far-UV CD spectra of these proteins refolded in the absence and presence of Ca^{2+} indicated that Δloop-Tk-subtilisin completely lost the ability to fold into a native structure. In contrast, two other proteins retained this ability, although their refolding rates were greatly decreased compared to that of Pro-S324A. Determination of the crystal structures of these proteins purified in a Ca^{2+}-bound form indicates that the structures of ΔCa2-Pro-S324A and ΔCa3-Pro-S324A are virtually identical to that of Pro-S324A, except that they lack the Ca2 and Ca3 sites, respectively, and the structure of the Ca^{2+}-binding loop is destabilized. Nevertheless, these proteins were slightly more stable than Pro-S324A. These results suggest that the Ca^{2+}-binding loop is required for folding of Tk-subtilisin but does not seriously contribute to the stabilization of Tk-subtilisin in a native structure.

Subtilisins and subtilisin-like serine proteases are synthesized as inactive precursors, which consist of a signal peptide, a propeptide, and a mature domain (*1*, *2*). While signal peptides act as a signal for transport, propeptides function as an intramolecular chaperone that assists folding of their cognate mature domains (*3*−*8*). Without propeptide, the mature domain is folded into an inactive form with a molten globule-like structure (*9*−*12*). Propeptides also function as a potent inhibitor of their cognate mature domains (*13*−*16*). Therefore, not only folding of the mature domain but also subsequent autoprocessing and degradation of the propeptide are required for generation of an active protease molecule. This maturation mechanism has also been observed for other prokaryotic and eukaryotic proteases, including a serine protease (*17*), aspartic proteases (*18*, *19*), cysteine proteases (*20*, *21*), and metalloproteases (*22*, *23*).

Tk-subtilisin from the hyperthermophiolic archaeon *Thermococcus kodakaraensis* is a highly thermostable serine protease with a half-life of 50 min at 100 °C (*24*, *25*). Tk-subtilisin (Gly70−Gly398) matures from Pro-Tk-subtilisin[1] (Gly1−Gly398) upon autoprocessing and degradation of Tk-propeptide (Gly1−Leu69) (*25*). Tk-propeptide functions not only as an intramolecular chaperone (*26*, *27*) but also as a strong inhibitor (*25*, *28*, *29*) of Tk-subtilisin. However, the maturation process of Tk-subtilisin is different from those of other subtilisins and subtilisin-like serine proteases in terms of the requirement of Ca^{2+} for folding of the mature domain. Tk-subtilisin requires Ca^{2+} for folding and assumes a molten globule-like structure in the absence of Ca^{2+} even in the presence of Tk-propeptide (*26*). In contrast, bacterial subtilisins and their homologues do not require Ca^{2+} for folding but require it for stability (*30*−*34*).

The crystal structure of Tk-subtilisin (*27*, *35*) strongly resembles those of bacterial subtilisins (*36*−*38*), except that it has a unique insertion of a long Ca^{2+}-binding loop (Gly206−Glu229) between the α6m-helix and the β5m-strand (Figure 1). This loop contains four Ca^{2+}-binding sites (Ca2−Ca5). Because the α6m-helix, β5m-strand, and α7m-helix form a central αβα-substructure, and formation of this αβα-substructure has been proposed to be crucial for folding of bacterial subtilisins (*39*, *40*), binding of the Ca^{2+} ions to this loop may be required to induce folding of a central αβα-substructure and thereby folding of an entire protein molecule. However, it remains to be determined whether this loop is required for folding of Tk-subtilisin.

In this report, we constructed three mutant proteins of Pro-Tk-subtilisin or its active site mutant Pro-S324A, all of which are

[†]This work was supported in part by a Grant (21380065) from the Ministry of Education, Culture, Sports, Science, and Technology of Japan and by an Industrial Technology Research Grant Program from the New Energy and Industrial Technology Development Organization (NEDO) of Japan.

[‡]Coordinates were deposited as Protein Data Bank entries 2ZWO for ΔCa2-Pro-S324A and 2ZWP for ΔCa3-Pro-S324A.

*To whom correspondence should be addressed. Telephone and fax: +81-6-6879-7938. E-mail: kanaya@mls.eng.osaka-u.ac.jp.

[1]Abbreviations: Pro-Tk-subtilisin, subtilisin homologue from *Thermococcus kodakaraensis* in a pro form (Gly1−Gly398); Δloop-Tk-subtilisin, Pro-Tk-subtilisin with the Ca^{2+}-binding loop (Pro207−Asp226) deleted and the Gly206 → Asn, Ala228 → Met, and Glu229 → Asp mutations; Pro-S324A, Pro-Tk-subtilisin with the Ser324 → Ala mutation; ΔCa2-Pro-S324A, Pro-S324A with the Asp226 → Ala mutation; ΔCa3-Pro-S324A, Pro-S324A with the Asp225 → Ala mutation; DSC, differential scanning calorimetry; PDB, Protein Data Bank.

Published on Web 10/08/2009

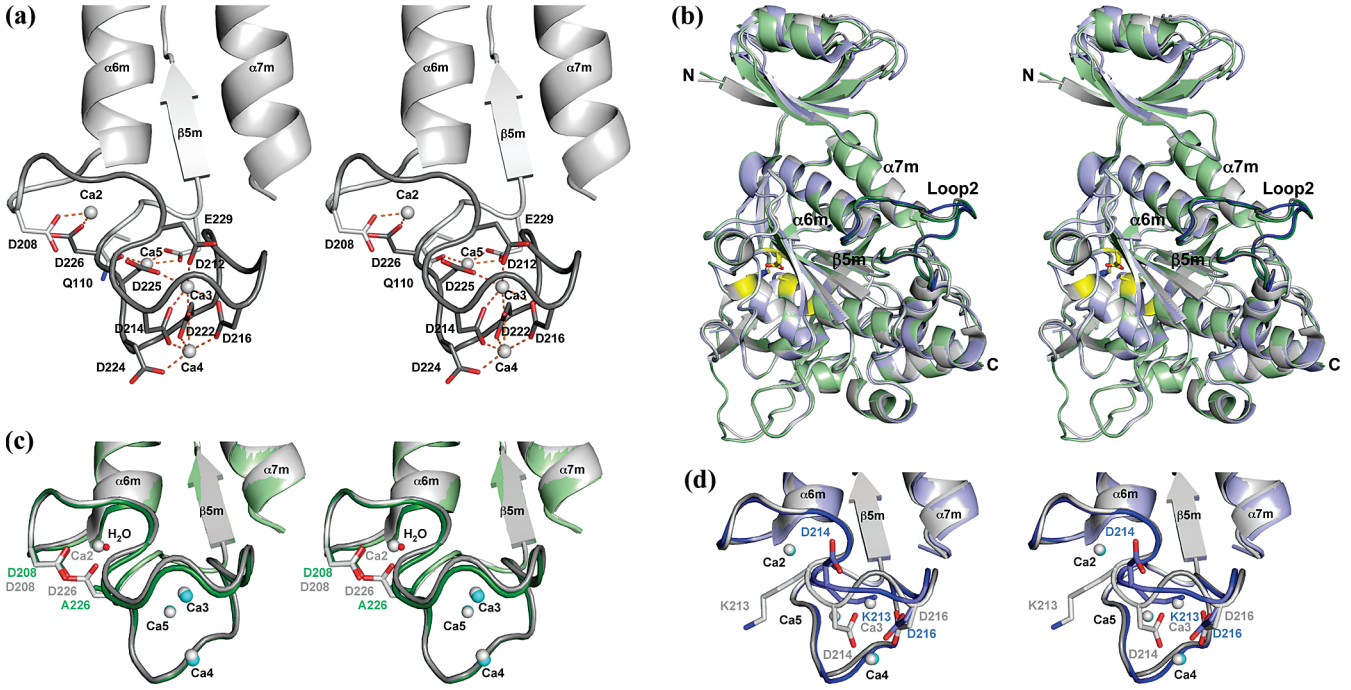

FIGURE 1: Stereoview of the crystal structures of ΔCa2-Pro-S324A and ΔCa3-Pro-S324A. (A) Structure of Pro-S324A (PDB entry 2E1P) around the Ca^{2+}-binding loop. The Ca^{2+}-binding loop is colored dark gray. The side chains of the amino acid residues that coordinate with the Ca^{2+} ions at the Ca2−Ca5 sites are shown in stick models, in which the oxygen atom is colored red. The Ca^{2+} ions are shown as light gray spheres. The positions of the β5m-strand and α6m- and α7m-helices are indicated. (B) Entire structures of ΔCa2-Pro-S324A (green) and ΔCa3-Pro-S324A (blue) superimposed on that of Pro-S324A (gray). Two active site residues (Asp115 and His153) and Ala324, which is substituted for the active site serine residue, are represented with yellow stick models, in which the oxygen and nitrogen atoms are colored red and blue, respectively. N and C represent the N- and C-termini, respectively. The Ca^{2+}-binding loop (Loop2) is indicted by a dark color. The positions of the β5m-strand and α6m- and α7m-helices are indicated. The Ca^{2+} ions are not shown for the sake of simplicity. (C) Structure of ΔCa2-Pro-S324A (green) around the Ca^{2+}-binding loop superimposed on that of Pro-S324A (gray). The side chains of Asp208 and Asp226 (Ala226 for ΔCa2-Pro-S324A) are indicated by stick models, in which the oxygen atom is colored red. The oxygen atom of the water molecule is also colored red. The Ca^{2+} ions bound to Pro-S324A and ΔCa2-Pro-S324A are shown as gray and cyan spheres, respectively. (D) Structure of ΔCa3-Pro-S324A (blue) around the Ca^{2+}-binding loop superimposed on that of Pro-S324A (gray). The side chains of Lys213, Asp214, and Asp216 are represented by stick models. The Ca^{2+} ions bound to Pro-S324A and ΔCa3-Pro-S324A are shown as gray and cyan spheres, respectively.

designed to remove the Ca^{2+}-binding loop, Ca2 site, or Ca3 site, overproduced in *Escherichia coli*, purified, and analyzed for structure, stability, and folding. On the basis of these results, we discuss the role of the Ca^{2+}-binding loop for folding of Tk-subtilisin.

MATERIALS AND METHODS

Plasmid Construction. The pET25b derivative for overproduction of Δloop-Tk-subtilisin, in which the unique insertion sequence of Tk-subtilisin (Pro207−Asp226) is removed and Gly206, Ala228, and Glu229 are replaced with Asn, Met, and Asp, respectively, was constructed using the polymerase chain reaction (PCR) overlap extension method (*41*). The pET25b derivative for overproduction of Pro-Tk-subtiisin (*25*) was used as a template. The sequences of the PCR primers are 5′-AATCCCTGCACATATGGGAGAGCAGAATACAATA-3′ for primer 1, 5′-GCTTATGACGTCCATTGCATTGAGAA-TGGCCTGC-3′ for primer 2, 5′-CCTCAATGCAATGGACG-TCATAAGCATGTCCC-3′ for primer 3, and 5′-AGTGGATC-CAATCAGCCCAGGGC-3′ for primer 4, where the *Nde*I (primer 1) and *Bam*HI (primer 4) sites are underlined. Primers 1 (forward) and 2 (reverse) were used to amplify the gene encoding Gly1−Asn206 of Pro-Tk-subtilisin. Primers 3 (forward) and 4 (reverse) were used to amplify the gene encoding Ala227−Gly398 of Pro-Tk-subtilisin. The two resultant PCR fragments were combined and amplified by PCR using primers 1 and 4. The PCR product was ligated into the *Nde*I and *Bam*HI sites of pET25b (Novagen).

The pET25b derivatives for overproduction of ΔCa2-Pro-S324A and ΔCa3-Pro-S324A, in which Asp226 and Asp225 of Pro-S324A are replaced with Ala, were constructed by PCR using the QuickChange II site-directed mutagenesis kit (Stratagene). The pET25b derivative for overproduction of the active site mutant of Pro-Tk-subtilisin, Pro-S324A (*42*), was used as a template. The PCR primers were designed such that the codons for Asp225 and Asp226 are changed from GAC to GCC for Ala and GAT to GCT for Ala, respectively. All DNA oligomers were synthesized by Hokkaido System Science. PCR was performed using a thermal cycler (Gene Amp PCR system 2400, Applied Biosystems) and KOD DNA polymerase (Toyobo). The DNA sequences were confirmed with an ABI Prism 310 DNA sequencer (Applied Biosystems).

Overproduction and Purification. Overproduction of Δloop-Tk-subtiisin, ΔCa2-Pro-S324A, and ΔCa3-Pro-S324A in *E. coli* in inclusion bodies and purification of these proteins in a urea-denatured form were conducted as described previously for Pro-S324A (*26*). These proteins were refolded either by being dialyzed against 20 mM Tris-HCl (pH 7.0) at 4 °C or 20 mM Tris-HCl (pH 7.0) containing 10 mM $CaCl_2$ and 1 mM DTT at 4 °C for 5 days. For purification of these proteins in a Ca^{2+}-bound form, the proteins refolded in the presence of Ca^{2+} were digested with chymotrypsin at 30 °C for 1 h at an enzyme:substrate ratio of 1:100 (w/w), incubated at 80 °C for 30 min, and centrifuged at

30000*g* for 30 min at 4 °C. The resultant supernatant was loaded onto a Sephacryl S-200HR column (GE Healthcare) equilibrated with 20 mM Tris-HCl (pH 7.0) containing 10 mM $CaCl_2$ and 50 mM NaCl. The fractions containing the protein were collected and dialyzed against 20 mM Tris-HCl (pH 7.0) containing 10 mM $CaCl_2$.

The protein concentration was determined from UV absorption using a cell with an optical path length of 1 cm on the basis of the fact that the absorbance of a 0.1% (1 mg/mL) solution at 280 nm is 1.31 for Δloop-Tk-subtilisin and 1.25 for ΔCa2-Pro-S324A and ΔCa3-Pro-S324A. These values were calculated by using absorption coefficients of 1526 M^{-1} cm^{-1} for tyrosine and 5225 M^{-1} cm^{-1} for tryptophan at 280 nm (*43*). The purity of the protein was analyzed via 12% sodium dodecyl sulfate−polyacrylamide gel electrophoresis (SDS−PAGE) (*44*), followed by staining with Coomassie Brilliant Blue (CBB).

Circular Dichroism Spectroscopy. The far-UV (200−260 nm) circular dichroism (CD) spectrum of the protein was measured with a J-725 automatic spectropolarimeter (Japan Spectroscopic Co.) at 20 °C. The buffer consisted of 20 mM Tris-HCl (pH 7.0), 10 mM $CaCl_2$, and 50 mM NaCl for the protein refolded in the presence of Ca^{2+} and 20 mM Tris-HCl (pH 7.0) for the protein refolded in the absence of Ca^{2+}. The protein concentration and optical path length were 0.15 mg/mL and 2 mm, respectively. The mean residue ellipticity, $[\theta]$, which has units of degrees square centimeters per decimole, was calculated by using an average amino acid molecular weight of 110.

Crystallization, Data Collection, Structure Determination, and Refinement. ΔCa2-Pro-S324A and ΔCa3-Pro-S324A purified in a Ca^{2+}-bound form (10 mg/mL) were dialyzed against 5 mM Tris-HCl (pH 7.0) and used for crystallization. ΔCa2-Pro-S324A was crystallized using the sitting-drop vapor-diffusion method at 4 °C as described previously (*27*). Crystals appeared after 2 weeks using 0.1 M MES (pH 6.5) containing 12% (w/v) PEG20000 (Crystal Screen II, Hampton Research). ΔCa3-Pro-S324A was crystallized using the hanging-drop method at 20 °C as described previously (*35*). Platelike overlapping poly crystals suitable for X-ray diffraction analysis appeared after 5 days using 0.1 M MES (pH 7.0) containing 12% (w/v) PEG8000. One of the single crystals separated from them was used for data collection. All crystals were soaked for 5 s in the cryobuffers containing 18% (v/v) ethylene glycol (Hampton Research) before being flash-frozen in a stream of nitrogen gas at −173 °C.

X-ray diffraction data were collected at a wavelength of 1.0 Å with the beamline BL38B1 station at SPring-8. Diffraction data were indexed, integrated, and scaled using the HKL2000 program suite (*45*). The crystal structure was determined by molecular replacement method using MOLREP (*46*) in the CCP4 program suite. The 2.3 Å structure of Pro-S324A (PDB entry 2E1P) was used as a starting model. Model building and refinement of the structure were completed using O (*47*) and CNS (*48*). Progress in the structure refinement was evaluated at each stage by the R_{free} value and by inspection of stereochemical parameters calculated with PROCHECK (*49*). The Ramachandran plot produced by PROCHECK showed that almost all residues in the structure were in the favored region. The statistics for data collection and refinement are listed in Table 1. The figures were prepared with PyMol (http://www.pymol.org).

Protein Data Bank Entry. The coordinates and structure factors have been deposited in the RCSB Protein Data Bank as entries 2ZWO for ΔCa2-Pro-S324A and 2ZWP for ΔCa3-Pro-S324A.

Table 1: Data Collection and Refinement Statistics

	ΔCa2-Pro-S324A	ΔCa3-Pro-S324A
wavelength (Å)	1.0	1.0
space group	$P2_12_12_1$	$P2_12_12_1$
cell parameters		
a, *b*, *c* (Å)	93.73, 118.31, 120.63	50.58, 87.74, 155.49
α, *β*, *γ* (deg)	90.0, 90.0, 90.0	90.0, 90.0, 90.0
no. of molecules per asymmetric unit	3	2
resolution range (Å)	50.0−2.07	50.0−2.40
no. of reflections measured	503222	161567
no. of unique reflections	82390	27872
completeness (%)	96.4 (84.3)[a]	94.5 (74.3)[a]
R_{merge} (%)[b]	8.9 (51.1)[a]	14.0 (43.3)[a]
average $I/\sigma(I)$	17.4 (1.3)[a]	11.9 (2.3)[a]
	Refinement	
resolution limits (Å)	50.0−2.07	50.0−2.40
no. of atoms		
protein/water/Ca^{2+}	8635/749/16	5674/418/11
R_{work} (%)	18.4	15.7
R_{free} (%)[c]	22.7	20.2
root-mean-square deviation from ideal values		
bond lengths (Å)	0.022	0.022
bond angles (deg)	2.086	2.121
average *B* factor (Å^2)		
protein	36.4	23.5
water/Ca^{2+}	41.8/38.9	30.0/28.1
Ramachandran plot		
most favored regions (%)	86.9	87.0
additional allowed regions (%)	12.9	12.7
generously allowed regions (%)	0.2	0.3

[a]Values in parentheses are for the highest-resolution shell. [b]$R_{merge} = \sum|I_{hkl} - \langle I_{hkl}\rangle|/\sum I_{hkl}$, where I_{hkl} is an intensity measurement for reflections with indices *hkl* and $\langle I_{hkl}\rangle$ is the mean intensity for multiply recorded reflections. [c]R_{free} was calculated using 5% of the total reflections chosen randomly and omitted from the refinement.

Determination of the Refolding Rate. The protein was denatured with 6 M guanidine hydrochloride (GdnHCl), refolded by dilution, incubated at 30 °C, and digested with chymotrypsin at appropriate intervals to remove the protein incorrectly folded or folded into a molten globule-like structure, as described previously (*27*). The amount of the protein, which is correctly folded and resistant to chymotryptic digestion, was estimated from the intensity of the band visualized with CBB staining following 12% SDS−PAGE, using Scion Image. The refolding yield was calculated by dividing the amount of protein correctly folded with that refolded in the absence of Ca^{2+}. The plot of the refolding yield as a function of the incubation time gave a refolding curve, which was used to determine the refolding rate.

DSC Measurements. Differential scanning calorimetry (DSC) was conducted using a VP-capillary DSC platform (Microcal) up to 130 °C at a scan rate of 1.0 °C/min. For the measurement, the protein (0.3 mg/mL) was dialyzed against 50 mM Tris-HCl (pH 8.5). All samples were filtered through a 0.22 *μ*m pore size membrane and degassed prior to the measurements.

RESULTS AND DISCUSSION

Mutant Design. The Ca^{2+}-binding loop of Tk-subtilisin (Gly206−Glu229), which is mostly formed by a unique insertion sequence of Tk-subtilisin (Pro207−Asp226), contains four Ca^{2+} ions (Figure 1). These Ca^{2+} ions are hexacoordinated with Asp208, Asp226, two main chain carbonyl oxygen atoms, and two water molecules in the Ca2 site, Asp212, Asp214, Asp216, Asp222, Asp225, and one main chain carbonyl oxygen atom in the Ca3 site, and Asp214, Asp216, Asp222 (bidentate), Asp224, and one water molecule in the Ca4 site, and heptacoordinated with Gln110, Glu229 (bidentate), two main chain carbonyl oxygen atoms, and two water molecules in the Ca5 site. Of these four Ca^{2+}-binding sites, the Ca2 and Ca3 sites seem to be more important for folding of the Ca^{2+}-binding loop than two other sites, because the Ca2 site brings the N- and C-terminal regions of this loop close to each other and the Ca3 site is located in the central region of this loop and coordinates with five aspartic acid residues. Therefore, two Pro-S324A derivatives, termed ΔCa2-Pro-S324A and ΔCa3-Pro-S324A, in which Asp226 and Asp225 of Pro-S324A are replaced with Ala, respectively, were constructed. Pro-S324A represents the active site mutant of Pro-Tk-subtilisin, in which Ser324 is replaced with Ala. Pro-S324A was used to construct these mutant proteins to prevent their autoprocessing and self-degradation. In addition, the Pro-Tk-subtilisin derivative, termed Δloop-Tk-subtilisin, in which the unique insertion sequence of Tk-subtilisin (Pro207−Asp226) is removed and Gly206, Ala228, and Glu229 are replaced with Asn, Met, and Asp, respectively, was constructed. These three mutations were introduced into Δloop-Tk-subtilisin to make the sequence of its loop connecting the α6m-helix and β5m-strand (Asn-Ala-Met-Asp) similar to those of bacterial subtilisins (e.g., Asn-Asn-Met-Asp for subtilisins E and BPN′).

Overproduction and Purification of the Mutant Proteins. ΔCa2-Pro-S324A, ΔCa3-Pro-S324A, and Δloop-Tk-subtilisin were overproduced in *E. coli* and purified in a urea-denatured form to give a single band on SDS−PAGE (data not shown). These proteins were refolded either in the presence or in the absence of Ca^{2+}. The proteins refolded in the absence of Ca^{2+} were defined as those in a Ca^{2+}-free form, while the proteins refolded in the presence of Ca^{2+}, treated with chymotrypsin, and purified by Sephacryl S-200HR column chromatography were defined as those in a Ca^{2+}-bound form. It has previously been shown that Pro-S324A in a Ca^{2+}-bound form is highly resistant to chymotryptic digestion, while Pro-S324A in a Ca^{2+}-free form is highly sensitive to it (*26*). ΔCa2-Pro-S324A and ΔCa3-Pro-S324A were purified both in a Ca^{2+}-free and Ca^{2+}-bound form, while Δloop-Tk-subtilisin was purified only in a Ca^{2+}-free form. Δloop-Tk-subtilisin in a Ca^{2+}-bound form was not purified, because the protein was completely digested by chymotrypsin even when it was refolded in the presence of Ca^{2+}. The purification yields of these proteins in a Ca^{2+}-free form were comparable to that of Pro-S324A, while those of ΔCa2-Pro-S324A and ΔCa3-Pro-S324A in a Ca^{2+}-bound form were lower than that of Pro-S324A by approximately 5-fold.

CD Spectra of the Mutant Proteins. It has been reported that the far-UV CD spectrum of Pro-S324A is changed, such that the wavelength at which it gives the minimum CD value is shifted from 208 to 222 nm, when the conformation of pro-S324A is changed from a molten globule-like structure to a native structure upon Ca^{2+} binding (*26*). To examine whether the conformation of the mutant proteins is changed equally upon Ca^{2+} binding, the far-UV CD spectra of the mutant proteins were measured. The far-UV CD spectra of ΔCa2-Pro-S324A and ΔCa3-Pro-S324A refolded in the absence of Ca^{2+} gave a broad trough with the minimum at around 208 nm, while those refolded in the presence of Ca^{2+} gave it at around 222 nm (Figure 2). The spectra of ΔCa3-Pro-S324A refolded in the presence and absence of Ca^{2+} are not shown in Figure 2, because they are highly similar to those of ΔCa2-Pro-S324A. The spectra of these proteins refolded in the absence and presence of Ca^{2+} are nearly identical to those of Pro-S324A in a Ca^{2+}-free form and a Ca^{2+}-bound form, respectively (data not shown). These results suggest that the mutation at Asp225 or Asp226 does not seriously affect not only the conformation of Pro-S324A either in a Ca^{2+}-free form or a Ca^{2+}-bound form but also the ability of pro-S324A to fold into a native structure. In contrast, the far-UV CD spectrum of Δloop-Tk-subtilisin refolded in the presence of Ca^{2+} was nearly identical to that refolded in the absence of Ca^{2+} (Figure 2). Both spectra strongly resemble those of ΔCa2-Pro-S324A and ΔCa3-Pro-S324A in a Ca^{2+}-free form. These results suggest that removal of the Ca^{2+}-binding loop does not seriously affect the conformation of Pro-S324A in a Ca^{2+}-free form but causes complete loss of the ability of pro-S324A to fold into a native structure.

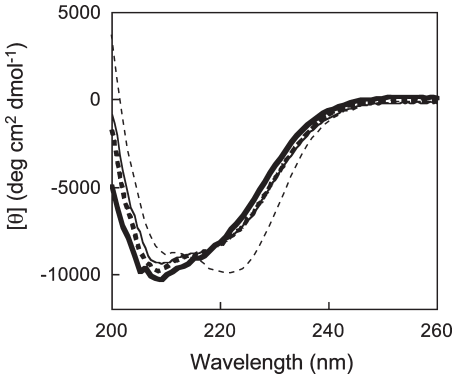

FIGURE 2: Far-UV CD spectra of Δloop-Tk-subtilisin refolded in the presence (dashed thick line) and absence (solid thin line) of Ca^{2+} and ΔCa2-Pro-S324A refolded in the presence (dashed thin line) and absence (solid thick line) of Ca^{2+}. The spectra were recorded at 20 °C and pH 7.0.

Crystal Structures of ΔCa2-Pro-S324A and ΔCa3-Pro-S324A. To examine whether ΔCa2-Pro-S324A and ΔCa3-Pro-S324A purified in a Ca^{2+}-bound form assume a native structure but lack the Ca2 or Ca3 site, their crystal structures were determined at 2.1 and 2.4 Å resolution, respectively. The asymmetric unit of the ΔCa2-Pro-S324A structure consists of three molecules (molecules A−C). Molecule A contains 395 of 398 residues, with three N-terminal residues missing. Molecule B contains 393 of 398 residues, with one N-terminal residue and four residues from Leu75 to Gly78 missing. Molecule C contains 389 of 398 residues, with three N-terminal residues and six residues from Leu75 to Thr80 missing. These structures are virtually identical with one another with root-mean-square deviation (rmsd) values of 0.56 Å between molecules A and B, 0.46 Å between molecules A and C, and 0.55 Å between molecules B and C, for 389 Cα atoms. We used the structure of molecule A as a representative. The asymmetric unit of the ΔCa3-Pro-S324A structure consists of two molecules (molecules A and B). Molecule A contains 389 of 398 residues, with four N-terminal residues and five residues from Gly76 to Thr80 missing. Molecule B contains 383 of 398 residues, with one N-terminal residue, five residues from Gly76 to Thr80, and nine

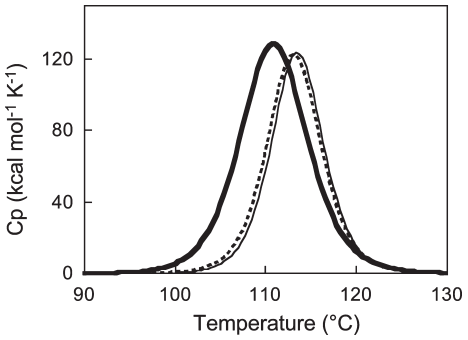

FIGURE 3: Excess heat capacity curves of Pro-S324A (solid thick line), ΔCa2-Pro-S324A (solid thin line), and ΔCa3-Pro-S324A (dashed thick line) measured at a scan rate of 1 °C/min. The proteins were dissolved in 50 mM Tris-HCl (pH 8.5) at 0.3 mg/mL.

residues from Lys213 to Gly221 missing. These two structures are virtually identical with each other with an rmsd value of 0.76 Å for 383 Cα atoms. We used the structure of molecule A as a representative.

The overall structures of ΔCa2-Pro-S324A and ΔCa3-Pro-S324A are superimposed onto that of Pro-S324A in Figure 1B. These structures are virtually identical with that of Pro-S324A with rmsd values of 0.50−0.51 Å for 389 Cα atoms, except that they lack the Ca2 or Ca3 site. The structure of ΔCa2-Pro-S324A around the Ca^{2+}-binding loop is superimposed onto that of Pro-S324A in Figure 1C. In the ΔCa2-Pro-S324A structure, one water molecule is located at the position corresponding to the Ca2 site. This water molecule is located at the same position in the other structures with two molecules per asymmetric unit as well. The structure of ΔCa3-Pro-S324A around the Ca^{2+}-binding loop is superimposed onto that of Pro-S324A in Figure 1D. This structure lacks the Ca3 site. However, in this structure, the side chain of Lys213 is greatly shifted such that its ε-amino group is located at the position corresponding to the Ca3 site. The positive charge of the ε-amino group of Lys213 may stabilize the structure of the Ca^{2+}-binding loop by weakening negative charge repulsions among acidic residues as a substitute of the Ca^{2+} ion. In contrast, the Lys213−Gly221 region is disordered in the structure of another molecule (molecule B) per asymmetric unit (data not shown). As a result, this structure lacks the Ca4 site as well.

The average *B* factor of the amino acid residues that make up most of the Ca^{2+}-binding loop (Gly209−Asp226) relative to that consisting of a central αβα-substructure (Gly191−Asp208 and Ala227−Ala254) was calculated to be 1.12 for Pro-S324A, 1.36 for ΔCa2-Pro-S324A, and 1.64 for ΔCa3-Pro-S324A. These results suggest that the structure of the Ca^{2+}-binding loop is destabilized by removal of the Ca2 or Ca3 site, but more seriously by removal of the Ca3 site.

Thermal Stability. To examine whether removal of the Ca2 or Ca3 site affects the stability of Pro-S324A, heat-induced unfolding of ΔCa2-Pro-S324A and ΔCa3-Pro-S324A in a Ca^{2+}-bound form was analyzed by differential scanning calorimetry (DSC) under a condition similar to that for X-ray crystallographic analysis. Because the thermal unfolding of these proteins was not reversible under any condition examined, the thermodynamic parameters for unfolding of these proteins could not be determined. However, the thermal unfolding curves of these proteins, which showed a single transition, were reproducible, unless the condition for the measurement was significantly changed (Figure 3). The melting temperatures (T_m) of these proteins were 111 ± 0.023 °C for Pro-S324A, 114 ± 0.022 °C for ΔCa2-Pro-S324A, and 113 ± 0.022 °C for ΔCa3-Pro-S324A. These results indicate that removal of the Ca2 or Ca3 site does not decrease the stability of Pro-S324A but rather slightly increases it.

It is noted that the pH of the Tris-HCl buffer used for DSC analysis might be significantly shifted from pH 8.5 at around 110 °C. However, it is unlikely that Pro-S324A and its derivatives are denatured because of the pH shift, because these proteins are highly stable over a wide pH range from 2 to 12 (S. Tanaka, personal communication).

Refolding Rate. To examine whether removal of the Ca2 or Ca3 site affects the rate of refolding of Pro-S324A, refolding of ΔCa2-Pro-S324A and ΔCa3-Pro-S324A was kinetically analyzed by terminating the refolding reaction with appropriate intervals and determining the amount of correctly folded protein. The spectroscopic method using fluorescence and CD cannot be used for this analysis, because this method cannot distinguish between refolding of the protein from a denatured state to a native state and that from a denatured state to a molten globule-like state. ΔCa2-Pro-S324A and ΔCa3-Pro-S324A were denatured with 6 M GdnHCl, diluted with the buffer containing 10 mM $CaCl_2$ by 100-fold for refolding, and incubated at 30 °C. With appropriate intervals, the refolding reaction was terminated by the addition of 10 mM EDTA, and the protein incorrectly folded or folded into a molten globule-like structure was digested with chymotrypsin. The SDS−PAGE analyses indicated that the amount of correctly refolded protein of ΔCa2-Pro-S324A or ΔCa3-Pro-S324A, which is resistant to chymotryptic digestion, increases much more slowly than that of Pro-S324A (Figure 4A). The result of ΔCa3-Pro-S324A is not shown in Figure 4A, because it is similar to that of ΔCa2-Pro-S324A. The refolding curves of these proteins could be fitted to a single-exponential process with rate constants of 1.3 ± 0.13 min^{-1} for Pro-S324A, 0.020 ± 0.0022 min^{-1} for ΔCa2-Pro-S324A, and 0.019 ± 0.0023 min^{-1} for ΔCa3-Pro-S324A (Figure 4B). These results indicate that the refolding rate of Pro-S324A is greatly reduced by removal of the Ca2 or Ca3 site.

It is noted that S324A-subtilisin, which represents the active site mutant of Tk-subtilisin, is refolded with a rate constant of 1.8 min^{-1} in the presence of Tk-propeptide (*27*). This rate is higher than that of Pro-S324A, probably because S324A-subtilisin is refolded in the presence of Tk-propeptide with a folded structure. It has been reported that the ability of propeptide to accelerate subtilisin folding is correlated with its stability (*50*). In addition, the presence of an excess of Tk-propeptide (2:1 propeptide:subtilisin molar ratio) might give rise to a refolding rate higher than that of Pro-S324A.

Role of the Ca^{2+}-Binding Loop. The Ca^{2+}-binding loop, which connects the α6m-helix and β5m-strand, is rich in Asp (Figure 1A). This loop is probably unfolded in the absence of Ca^{2+}, due to extensive negative charge repulsions among aspartic acid residues. However, in the presence of Ca^{2+}, these aspartic acid residues come close with one another to form Ca^{2+}-binding sites and directly coordinate with the Ca^{2+} ions at these sites. As a result, the Ca^{2+}-binding loop is folded into a correct structure, which permits proper arrangement of the α6m-helix and β5m-strand and thereby folding of a central αβα-substructure (Figure 1B). However, removal of the Ca2 or Ca3 site destabilizes the structure of the Ca^{2+}-binding loop and greatly reduces the refolding rate of the protein without seriously affecting the stability of the entire protein molecule. Therefore, the Ca^{2+}-binding loop may be required to initiate folding of the mature

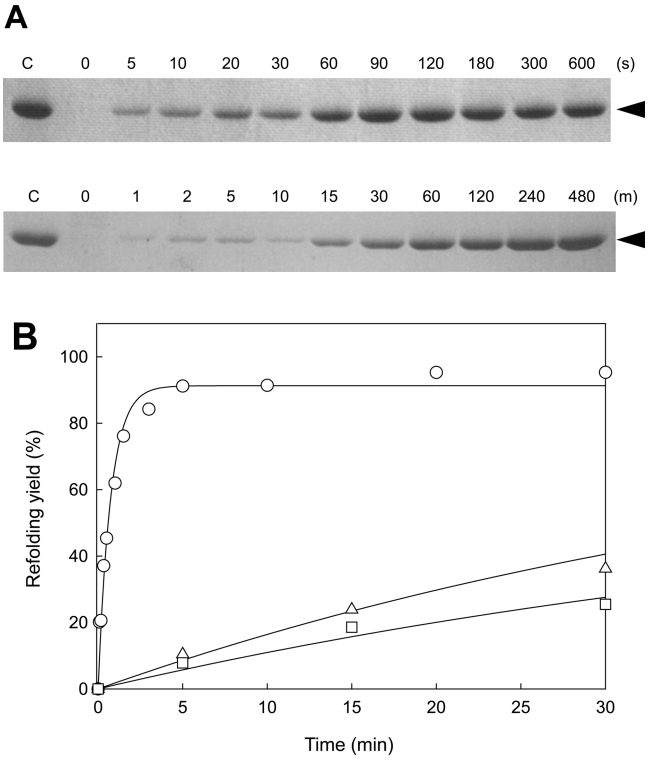

FIGURE 4: Refolding rates of ΔCa2-Pro-S324A and ΔCa3-Pro-S324A. (A) SDS−PAGE of the protein correctly refolded. Pro-S324A (top) and ΔCa2-Pro-S324A (bottom) were denatured with 6 M GdnHCl, diluted with 50 mM Tris-HCl (pH 8.0) containing 10 mM $CaCl_2$ and 1 mM DTT by 100-fold, and incubated at 30 °C for refolding. With appropriate intervals shown at the top of the gel, the refolded protein was digested with chymotrypsin and analyzed via 12% SDS−PAGE as described in Materials and Methods. The gel was stained with CBB. The position of Pro-S324A or ΔCa2-Pro-S324A is indicated by an arrowhead. Lane C contained Pro-S324A or ΔCa2-Pro-S324A refolded in the absence of Ca^{2+} (without chymotryptic digestion). (B) Refolding curves. The refolding yields of Pro-S324A (○), ΔCa2-Pro-S324A (△), and ΔCa3-Pro-S324A (□) are shown as a function of incubation time. The refolding yield was calculated by estimating the amount of correctly refolded protein from the intensity of the band visualized with CBB staining following SDS−PAGE. The line represents the optimal fit to the data.

domain. In fact, Δloop-Tk-subtilisin, which lacks the Ca^{2+}-binding loop, completely loses the ability to fold into a native structure. ΔCa2-Pro-S324A and ΔCa3-Pro-S324A do not completely lose this ability, probably because binding of the water molecule to the position corresponding to the Ca2 site and movement of the ε-amino group of Lys213 to the position corresponding to the Ca3 site compensate at least partly for the destabilization of the structure of the Ca^{2+}-binding loop caused by the removal of the Ca2 or Ca3 site.

We have previously shown that Tk-propeptide functions as an intramolecular chaperone (*27*). However, its chaperone function becomes weaker as the Ca^{2+} concentration increases. For example, it increases the refolding rate of Tk-subtilisin by approximately 10 times in the presence of 10 mM $CaCl_2$ and 100 times in the presence of 1 mM $CaCl_2$. In the absence of Tk-propeptide, the refolding rate of Tk-subtilisin increases as the Ca^{2+} concentration increases. These results suggest that Tk-propeptide assists folding of Tk-subtilisin, which is probably initiated by folding of the Ca^{2+}-binding loop, in an auxiliary manner. Tk-propeptide apparently assists folding of a central αβα-substructure. It has been reported that a high kinetic barrier between the unfolded and folded states ensures the proteolytic stability of the native structure and allows the extracellular protease to function in harsh environments (*51*). Because *T. kodakaraensis* grows even at 102 °C (*52*), the kinetic barrier for folding of Pro-Tk-subtilisin should be extremely higher than those of subtilisins and subtilisin-like serine proteases from mesophilic organisms. To reduce this unusual high kinetic barrier, folding of Pro-Tk-subtilisin may be assisted not only by the chaperone function of the propeptide domain but also by folding of the Ca^{2+}-binding loop.

ACKNOWLEDGMENT

We thank Dr. K. Yutani for performing differential scanning calorimetry and helpful suggestions. The synchrotron radiation experiments were performed at beamline BL38B1 in the SPring-8 with the approval of the Japan Synchrotron Radiation Research Institute (JASRI) (Proposal 2007B1119).

REFERENCES

1. Siezen, R. J., and Leunissen, J. A. M. (1997) Subtilases: The superfamily of subtilisin-like serine proteases. *Protein Sci. 6*, 501–523.
2. Khan, A. R., and James, M. N. (1998) Molecular mechanisms for the conversion of zymogens to active proteolytic enzymes. *Protein Sci. 7*, 815–836.
3. Shinde, U., and Inouye, M. (1996) Propeptide-mediated folding in subtilisin: The intramolecular chaperone concept. *Adv. Exp. Med. Biol. 379*, 147–154.
4. Sohl, J. L., Jaswal, S. S., and Agard, D. A. (1998) Unfolding conformations of α-lytic protease are stable than its native state. *Nature 395*, 817–819.
5. Marie-Claire, C., Yabuta, Y., Suefuji, K., Matsuzawa, H., and Shinde, U. P. (2001) Folding pathway mediated by an intramolecular chaperone: The structural and functional characterization of the aqualysin I propeptide. *J. Mol. Biol. 305*, 151–165.
6. Bryan, P. N. (2002) Prodomains and protein folding catalysis. *Chem. Rev. 102*, 4805–4816.
7. Fisher, K. E., Ruan, B., Alexander, P. A., Wang, L., and Bryan, P. N. (2007) Mechanism of the kinetically-controlled folding reaction of subtilisin. *Biochemistry 46*, 640–651.
8. Falzon, L., Patel, S., Chen, Y. J., and Inouye, M. (2007) Autotomic behavior of the propeptide in propeptide-mediated folding of pro-subtilisin E. *J. Mol. Biol. 366*, 494–503.
9. Eder, J., Rheinnecker, M., and Fersht, A. R. (1993) Folding of subtilisin BPN′: Characterization of a folding intermediate. *Biochemistry 32*, 18–26.
10. Eder, J., Rheinnecker, M., and Fersht, A. R. (1993) Folding of subtilisin BPN′: Role of the pro-sequence. *J. Mol. Biol. 233*, 293–304.
11. Shinde, U. P., and Inouye, M. (1995) Folding pathway mediated by an intramolecular chaperone: Characterization of the structural changes in pro-subtilisin E coincident with autoprocessing. *J. Mol. Biol. 252*, 25–30.
12. Anderson, D. E., Peters, R. J., Wilk, B., and Agard, D. A. (1999) α-Lytic protease precursor: Characterization of a structural folding intermediate. *Biochemistry 38*, 4728–4735.
13. Baker, D., Silen, J. L., and Agard, D. A. (1992) Protease pro region required for folding is a potent inhibitor of the mature enzyme. *Proteins 12*, 339–344.
14. Li, Y., Hu, Z., Jordan, F., and Inouye, M. (1995) Functional analysis of the propeptide of subtilisin E as an intramolecular chaperone for protein folding. Refolding and inhibitory abilities of propeptide mutants. *J. Biol. Chem. 270*, 25127–25132.
15. Yabuta, Y., Takagi, H., Inouye, M., and Shinde, U. (2001) Folding pathway mediated by an intramolecular chaperone: Propeptide release modulates activation precision of pro-subtilisin. *J. Biol. Chem. 276*, 44427–44434.
16. Basak, A., and Lazure, C. (2003) Synthetic peptides derived from the prosegments of proprotein convertase 1/3 and furin are potent inhibitors of both enzymes. *Biochem. J. 373*, 231–239.
17. Winther, J. R., and Sorensen, P. (1991) Propeptide of carboxypeptidase Y provides a chaperone-like function as well as inhibition of the enzymatic activity. *Proc. Natl. Acad. Sci. U.S.A. 88*, 9330–9334.
18. van den Hazel, H. B., Kielland-Brandt, M. C., and Winther, J. R. (1993) The propeptide is required for in vivo formation of stable active

yeast proteinase A and can function even when not covalently linked to the mature region. *J. Biol. Chem. 268*, 18002–18007.
19. Fukuda, R., Horiuchi, H., Ohta, A., and Takagi, M. (1994) The prosequence of *Rhizopus niveus* aspartic proteinase-I supports correct folding and secretion of its mature part in *Saccharomyces cerevisiae* *J. Biol. Chem. 269*, 9556–9561.
20. Carmona, E., Dufour, E., Plouffe, C., Takebe, S., Mason, P., Mort, J. S., and Ménard, R. (1996) Potency and selectivity of the cathepsin L propeptide as an inhibitor of cysteine proteases. *Biochemistry 35*, 8149–8157.
21. Smith, S. M., and Gottesman, M. M. (1989) Activity and deletion analysis of recombinant human cathepsin L expressed in *Escherichia coli*. *J. Biol. Chem. 264*, 20487–20495.
22. Marie-Claire, C., Ruffet, E., Beaumont, A., and Roques, B. P. (1999) The prosequence of thermolysin acts as an intramolecular chaperone when expressed in trans with the mature sequence in *Escherichia coli*. *J. Mol. Biol. 285*, 1911–1915.
23. Nirasawa, S., Nakajima, Y., Zhang, Z. Z., Yoshida, M., and Hayashi, K. (1999) Intramolecular chaperone and inhibitor activities of a propeptide from a bacterial zinc aminopeptidase. *Biochem. J. 131*, 25–31.
24. Kannan, Y., Koga, Y., Inoue, Y., Haruki, M., Takagi, M., Imanaka, T., Morikawa, M., and Kanaya, S. (2001) Active subtilisin-like protease from a hyperthermophilic archaeon in a form with a putative prosequence. *Appl. Environ. Microbiol. 67*, 2445–2552.
25. Pulido, M. A., Saito, K., Tanaka, S., Koga, Y., Morikawa, M., Takano, K., and Kanaya, S. (2006) Ca^{2+}-dependent maturation of Tk-subtilisin from a hyperthermophilic archaeon: Propeptide is a potent inhibitor of the mature domain but is not required for its folding. *Appl. Environ. Microbiol. 72*, 4154–4162.
26. Tanaka, S., Saito, K., Chon, H., Matsumura, H., Koga, Y., Takano, K., and Kanaya, S. (2007) Crystal structure of unautoprocessed precursor of subtilisin from a hyperthermophilic archaeon: Evidence for Ca^{2+}-induced folding. *J. Biol. Chem. 282*, 8246–8255.
27. Tanaka, S., Takeuchi, Y., Matsumura, H., Koga, Y., Takano, K., and Kanaya, S. (2008) Crystal structure of Tk-subtilisin folded without propeptide: Requirement of propeptide for acceleration of folding. *FEBS Lett. 582*, 3875–3878.
28. Pulido, M. A., Koga, Y., Takano, K., and Kanaya, S. (2007) Directed evolution of Tk-subtilisin from a hyperthermophilic archaeon: Identification of a single amino acid substitution in the propeptide region responsible for low-temperature adaptation. *Protein Eng., Des. Sel. 20*, 143–153.
29. Pulido, M. A., Tanaka, S., Sringiew, C., You, D.-J., Matsumura, H., Koga, Y., Takano, K., and Kanaya, S. (2007) Requirement of left-handed glycine residue for high stability of the Tk-subtilisin propeptide as revealed by mutational and crystallographic analyses. *J. Mol. Biol. 374*, 1359–1373.
30. Voordouw, G., Milo, C., and Roche, R. S. (1976) Role of bound calcium ions in thermostable, proteolytic enzymes. Separation of intrinsic and calcium ion contributions to the kinetic thermal stability. *Biochemistry 15*, 3716–3724.
31. Pantoliano, M. W., Whitlow, M., Wood, J. F., Dodd, S. W., Hardman, K. D., Rollence, M. L., and Bryan, P. N. (1989) Large increases in general stability for subtilisin BPN′ through incremental changes in the free energy of unfolding. *Biochemistry 28*, 7205–7213.
32. Gros, P., Kalk, K. H., and Hol, W. G. (1991) Calcium binding to thermitase. Crystallographic studies of thermitase at 0, 5, and 100 mM calcium. *J. Biol. Chem. 266*, 2953–2961.
33. Bryan, P., Alexander, P., Strausberg, S., Schwarz, F., Lan, W., Gilliland, G., and Gallagher, D. T. (1992) Energetics of folding subtilisin BPN′. *Biochemistry 31*, 4937–4945.
34. Smith, C. A., Toogood, H. S., Baker, H. M., Daniel, R. M., and Baker, E. N. (1999) Calcium-mediated thermostability in the subtilisin superfamily: The crystal structure of *Bacillus* Ak.1 protease at 1.8 Å resolution. *J. Mol. Biol. 294*, 1027–1040.
35. Tanaka, S., Matsumura, H., Koga, Y., Takano, K., and Kanaya, S. (2007) Four new crystal structures of Tk-subtilisin in unautoprocessed, autoprocessed and mature forms: Insights into structural changes during maturation. *J. Mol. Biol. 372*, 1055–1069.
36. Wright, C. S., Alden, R. A., and Kraut, J. (1969) Structure of subtilisin BPN′ at 2.5 Å resolution. *Nature 221*, 235–242.
37. Syed, R., Wu, Z. P., Hogle, J. M., and Hilvert, D. (1993) Crystal structure of selenosubtilisin at 2.0-Å resolution. *Biochemistry 32*, 6157–6164.
38. Jain, S. C., Shinde, U. P., Li, Y., Inouye, M., and Berman, H. M. (1998) The crystal structure of an autoprocessed Ser221Cys-subtilisin E-propeptide complex at 2.0 Å resolution. *J. Mol. Biol. 284*, 137–144.
39. Gallagher, T., Gilliland, G., Wang, L., and Bryan, P. (1995) The prosegment-subtilisin BPN′ complex: Crystal structure of a specific 'foldase'. *Structure 3*, 907–914.
40. Bryan, P., Wang, L., Hoskins, J., Ruvinov, S., Strausberg, S., Alexander, P., Almog, O., Gilliland, G. L., and Gallagher, T. (1995) Catalysis of a protein folding reaction: Mechanistic implications of the 2.0 Å structure of the subtilisin-prodomain complex. *Biochemistry 34*, 10310–10318.
41. Horton, R. M., Cai, Z. L., Ho, S. N., and Pease, L. R. (1990) Gene splicing by overlap extension: Tailor-made genes using the polymerase chain reaction. *BioTechniques 8*, 528–535.
42. Tanaka, S., Saito, K., Chon, H., Matsumura, H., Koga, Y., Takano, K., and Kanaya, S. (2006) Crystallization and preliminary X-ray diffraction study of an active-site mutant of pro-Tk-subtilisin from a hyperthermophilic archaeon. *Acta Crystallogr. F62*, 902–905.
43. Goodwin, T. W., and Morton, R. A. (1946) The spectrophotometric determination of tyrosine and tryptophan in proteins. *Biochem. J. 40*, 628–632.
44. Laemmli, U. K. (1970) Cleavage of structural proteins during the assembly of the head of bacteriophage T4. *Nature 227*, 680–685.
45. Otwinowski, Z., and Minor, W. (1997) Processing of X-ray diffraction data collected in oscillation mode. *Methods Enzymol. 276*, 307–326.
46. Vagin, A., and Teplyakov, A. (1997) MOLREP: An automated program for molecular replacement. *J. Appl. Crystallogr. 30*, 1022–1025.
47. Jones, T. A., Zou, J. Y., Cowan, S. W., and Kjeldgaard, M. (1991) Improved methods for building protein models in electron density maps and the location of errors in these models. *Acta Crystallogr. A47*, 110–119.
48. Brünger, A. T., Adams, P. D., Clore, G. M., DeLano, W. L., Gros, P., Grosse-Kunstleve, R. W., Jiang, J. S., Kuszewski, J., Nilges, M., Pannu, N. S., Read, R. J., Rice, L. M., Simonson, T., and Warren, G. L. (1998) Crystallography and NMR system (CNS): A new software suite for macromolecular structure determination. *Acta Crystallogr. D54*, 905–921.
49. Laskowski, R. A. (1993) PROCHECK: A program to check the stereochemical quality of protein structures. *J. Appl. Crystallogr. 26*, 283–291.
50. Wang, L., Ruan, B., Ruvinov, S., and Bryan, P. (1998) Engineering the independent folding of the subtilisin BPN′-pro-domain: Correlation of pro-domain stability with the rate of subtilisin folding. *Biochemistry 37*, 3165–3171.
51. Jaswal, S. S., Sohl, J. L., Davis, J. H., and Agard, D. A. (2002) Energetic landscape of α-lytic protease optimizes longevity through kinetic stability. *Nature 415*, 343–346.
52. Atomi, H., Fukui, T., Kanai, T., Morikawa, M., and Imanaka, T. (2004) Description of *Thermococcus kodakaraensis* sp. nov., a well studied hyperthermophilic archaeon previously reported as *Pyrococcus* sp. KOD1. *Archaea 1*, 263–267.